Fabrication of polystyrene microfluidic devices using a pulsed CO_2 laser system

Huawei Li · Yiqiang Fan · Rimantas Kodzius · Ian G. Foulds

Abstract In this article, we described a simple and rapid method for fabrication of droplet microfluidic devices on polystyrene substrate using a CO_2 laser system. The effects of the laser power and the cutting speed on the depth, width and aspect ratio of the microchannels fabricated on polystyrene were investigated. The polystyrene microfluidic channels were encapsulated using a hot-press bonding technique. The experimental results showed that both discrete droplets and laminar flows could be obtained in the device.

1 Introduction

During recent years, microfluidics has emerged as an advanced technique for analytical, biological, diagnostics and biomedical research (Jakeway et al. 2000, Nayak et al. 2008). As a subcategory of microfluidics, droplet microfluidics is very attractive for its potential to generate and manipulate discrete droplets in continuous flow, thus allowing for independent control of each droplet to act as microreactors that can be individually transported, mixed and analyzed (Link et al. 2006, Fair 2007).

Compared with conventional materials like silicon and glass, polymers have become more and more attractive to fabricate microfluidic devices because of their many advantages, such as low cost and ease of fabrication(Duffy et al. 1998, Dolink et al. 2000, Nayak et al. 2008). Many kinds of polymers have been used to fabricate microfluidic devices, such as Poly(methylmethacrylate) (PMMA) (Yao et al. 2009, Reedy et al. 2011), polystyrene (PS) (Darain et al. 2009, Young et al. 2011), polydimethylsiloxane (PDMS) (Hoek et al. 2010, Pla-Roca et al. 2011), polycarbonate (PC) (Ogonczyk et al. 2010, Jankowski et al. 2011) and PTFE (Fair 2007).

As one of the most widely used thermoplastics, polystyrene is low cost, optically transparent, inert and rigid (Chen et al. 2008). PS is well known for its resistivity against alcohols, polar solvents, diluted/concentrated acids (except HNO_3) and alkaline (Becker et al. 2000). Polystyrene is also widely used in molecular and cell biology due to its biocompatibility, being used for Petri dishes, test tubes, microplates, and other laboratory containers.

Furthermore, the surface of polystyrene can be readily functionalized (Kaur et al. 2008). For example, its surface can be easily transferred from hydrophobic to hydrophilic by various physical and chemical means, such as corona-discharge, irradiation and gas plasma (Chen. et al. 2008). Although the advantages make PS a very promising materials to fabricate microfluidic devices, the high investment in tools necessary to fabricate polystyrene microstructure precludes its adoption (Chen. et al. 2008).

Compared with the commonly used polymer microfabrication techniques such as hot-embossing (Martynova, et al. 1997, Gerlach et al. 2002), injection molding (Rotting et al. 2002), and photolithography (Lim et al. 2009), laser direct-writing micromachining is very promising because of its low-cost, fast speed and non-contact characteristics (Nayak 2008).

The laser ablation mechanism is usually a combination of photochemical and photothermal processes (Urech et al. 2010), in which some chemical bonds of the substance are broken directly due to photon absorption while others are thermally broken by the released heat from those excited molecules that do not break up photochemically. A CO_2 laser emits infrared radiation at a wavelength of 10.6 μm, which is not capable of directly breaking the chemical bonds, so that it is a totally

Huawei Li (✉)· Yiqiang Fan · Rimantas Kodzius · Ian G. Foulds
Department of Electrical Engineering, King Abdullah University of Science and Technology, Thuwal, KSA
Email: huawei.li@kaust.edu.sa
Tel: +966 2 8084389

photothermal mechanism for the CO_2 laser ablation process (Nayak 2008). CO_2 laser systems have been widely used for rapid production of microfluidic systems with polymers such as PMMA (Snakenborg et al. 2004, Yuan et al. 2007, Huang et al. 2010), PDMS (Liu et al. 2009, Huft et al. 2010), PC (Qi et al. 2009), and PTFE (Tolstopyatov 2005).

In this article, we investigated a low cost direct-writing laser ablation process to fabricate PS microfluidic devices without a replication template using a pulsed CO_2 laser system. The influence of the laser parameters, including laser power and cutting speed on the depth, width and aspect ratio was studied. Channels were capped with a second PS sheet via hot press bonding technique. This process significantly reduces the prototyping time and cost to fabricate PS-based microfluidic devices because of the elimination of masks, templates and the corresponding microfabrication, facilities and consumables, and it opens a door for fast development of PS-based microfluidic devices.

2 Experimental details

2.1 Materials

Polystyrene sheet with molecular weight of 267.8 kDa and thickness of 2 mm from Goodfellow Cambridge Limited, England was studied in this work as the microfluidic device substrate. Mineal oil (Sigma-Aldrich M5904) and 1% Cresol Red solution in DI water (w/w) with red color for visual clarity were used for the testing of the PS microfluidic device.

2.2 Apparatus

The laser ablation process was done by a commercially available CO_2 laser system (Universal PLS6.75, Universal Laser System Inc., AZ, USA). The CO_2 laser has a wavelength of 10.6 μm and a maximum output power of 75 W. The laser beam is focused by a lens with a focal length of 60 mm to a spot with a 0.127 mm diameter, and has an effective focal range of +/- 2.54 mm. The laser beam was guided by mirrors to the moving lens and these mirrors allowed the placement of laser beam to anywhere on the 813 cm by 457 cm working area (Universal Laser Systems User Guide).

The laser power can be set from 0 to 75 W along with the cutting speed from 0 to 300 mm/s by the Universal Control Panel program. The profile of the laser-cutting channel strongly depends on these two parameters.

The channel smoothness depends on PPI (pulses per inch) parameter. The laser beam is always pulsing during the work and the pulse number can be set between 1 and 1000 times per linear inch (PPI), regardless the cutting speed. We decided to use 1000 PPI, as it provided the smoothest channels for our experiments.

The micromachining pattern on the sample can be prepared by computer aided design programs, and CorelDraw was used in this work.

The profile of the microchannels was measured with a DEKTAK profiler system, and the cross-section images of the microchannels before and after bonding were obtained by SEM (FEI Quanta 600 FEG).

2.3 Fabrication of microchannels on polystyrene using CO_2 laser

A photothermal ablation process happens during the CO_2 laser cutting process (Klank et al. 2002). When the laser beam with certain power and cutting speed focuses on the surface of polystyrene sample, the temperature of the irradiated spot will increase rapidly, inducing melting, decomposition and vaporization of the material and leaving a void in the workpiece. The photothermal ablation process is depicted in Figure 1.

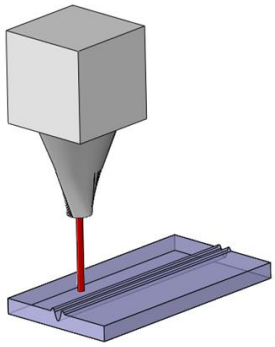

Fig. 1 Schematic diagram of the photothermal ablation process of CO_2 laser on polystyrene substrate

The profile of the laser cut microchannel depends on the intensity distribution of the laser beam, the laser power, cutting speed and the number of passes of the beam on the same channel. The material properties of the polystyrene, especially the thermal diffusivity and the decomposition mechanism, also play a critical role on the profile of the microchannel (Nayak, 2008).

The straight-line microchannel pattern on PS substrate was designed in the CorelDraw software and then printed with the Universal Control Panel program, which drove the laser system for the ablation process. The PS sheet was put on the laser cutting table, and the distance between the sample surface and the lens was fixed at 60 mm, to make sure that the laser focused on the sample surface and obtained minimum size of the laser beam.

To fabricate microchannels, the laser beam must have enough time to heat and vaporize polystyrene, otherwise only bump could be found on the surface of polystyrene. For example, when the cutting speed is 300 mm/s and the laser power is 0.4 W, the heat irradiated from the CO_2 laser can only form bump as shown in Figure 2. Microchannel starts to appear when the laser power is increased while the 300 mm/s cutting speed keeps constant, as shown in Figure 3. The minimum laser power and maximum cutting speed required to form a microchannel on polystyrene substrate with the CO_2 laser system are 3.0 W and 300 mm/s, and the channel depth is 1.8 μm.

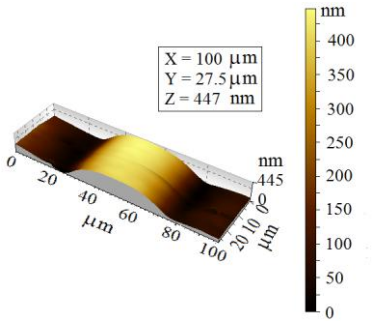

Fig. 2 AFM image of the irradiated area on polystyrene with laser power of 0.4 W and cutting speed of 300 mm/s

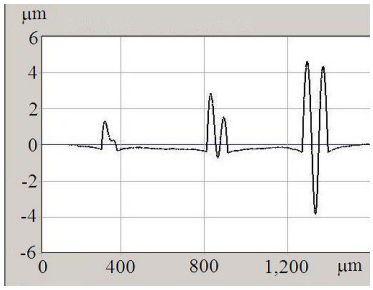

Fig. 3 Profiles of the polystyrene cross-microchannels formed with cutting speed of 300 mm/s and laser power of 1.5 W, 2.25 W and 3.8 W (from left to right)

To investigate the dependence of the microchannels on the laser power and cutting speed, various cutting speeds ranging from 10 mm/s to 52.5 mm/s were set in this work, and for each speed, the microchannels were fabricated using various laser powers ranging from 3.75 W to 33.75 W and PPI was always set to 1000. The tests were repeated 10 times to check the reproducibility of the laser ablation process and the dimension sizes of the microchannels were collected.

Figure 4 shows the plot of the depths of the microchannels as a function of the laser power with different cutting speeds on the polystyrene sheet, and the standard deviation of these data is 3%. It is clear that the depth of the microchannels increases with the increase of the laser power and the decrease of the laser cutting speed. With higher laser power and slower cutting speed, more heat will be applied on the polystyrene surface, resulting in a deeper molten pool. With a given cutting speed, the depth increases faster at low laser power, and then the slope becomes smaller and smaller.

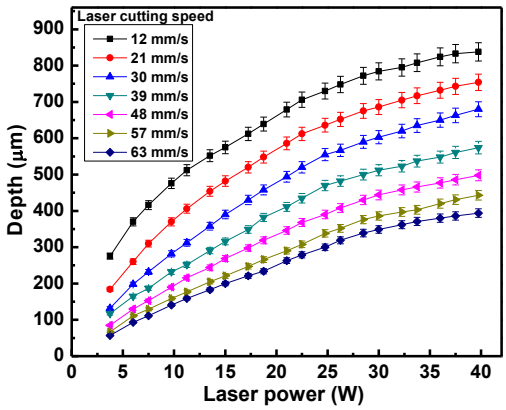

Fig. 4 Depths of the microchannels ablated with different laser powers and cutting speeds

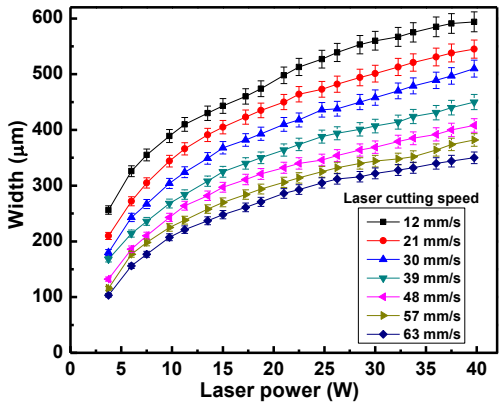

Fig. 5 Width of the microchannels ablated with different laser powers and cutting speeds

The widths of the microchannels are also plotted in Figure 5 as a function of the laser power with different cutting speeds and the standard deviation is also 3%. It can be seen that the width also depends on the laser power and cutting speed. Wider microchannels were fabricated at higher laser power and slower cutting speed, which is also because of the more heat on the polystyrene surface.

The aspect ratio (depth/width) is also an important factor to evaluate the micromachining quality of the microstructure. The result as shown in Figure 6 indicates that higher aspect ratio can be achieved using higher laser power and slower cutting speed. With a given cutting speed, higher aspect ratio is obtained with higher laser power; however, the aspect ratio could reach a saturated state when the laser power is high enough.

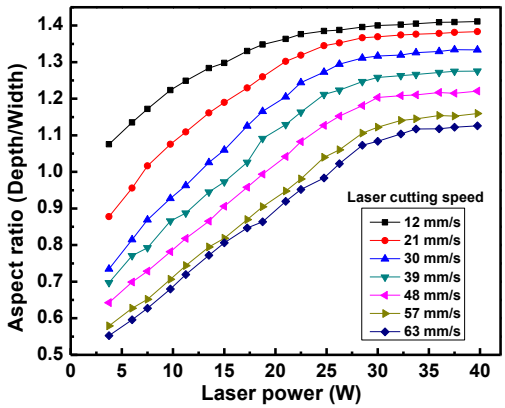

Fig. 6 Aspect ratio of the microchannels ablated with different laser powers and cutting speeds

The cross-section of the microchannel depends on the thermal diffusivity of the material and the intensity distribution within the laser beam. Since the thermal diffusivity of the polystyrene is as low as 10^{-3} cm^2/s (Huang et al. 2005), the microchannel's cross-section is mainly determined by the Gaussian distribution of laser intensity.

An example of such a Gaussian-like cross-section profile of the microchannel fabricated on the polystyrene substrate using laser power of 10 W and cutting speed of 50 mm/s is depicted in Figure 7(a), which can be explained by the Gaussian shape intensity distribution of the laser beam (Klank et al. 2002) and the small thermal diffusivity of polystyrene. We can see that the cutting process left small bumps on the edges of the microchannel, which are due to the surface tension driven flow of the molten polystyrene. Upon laser irradiation, a temperature gradient is created in the molten polystyrene, which decreases from the inner edge to the outer edge. Since the surface tension of polystyrene decreases with increasing temperature (Wu 1970), a surface tension gradient is also created, which will push the molten polystyrene towards the cooler region with higher surface tension (Chen et al. 2000). Confined by the solid edge of the polystyrene, the molten polystyrene accumulates and results in bumps during resolidification process. Compared with the depth, the bump height is small and all the bumps in our experiments were smaller than 50 μm.

The hot-press bonding of another piece of polystyrene cover plate on top of the laser-cutting sample was done by heating them together at 102 ^{o}C for 120 minutes, with a pressure of 4000 Pa on top of the cover plate to increase the contact force between the sample and the cover plate. The cross-section SEM image of the bonded sample is shown in Figure 7 (b). Although there were bumps on the edge of the microchannel before bonding, the cover plate was bonded with the sample very well, and there is no major deformation of the channel.

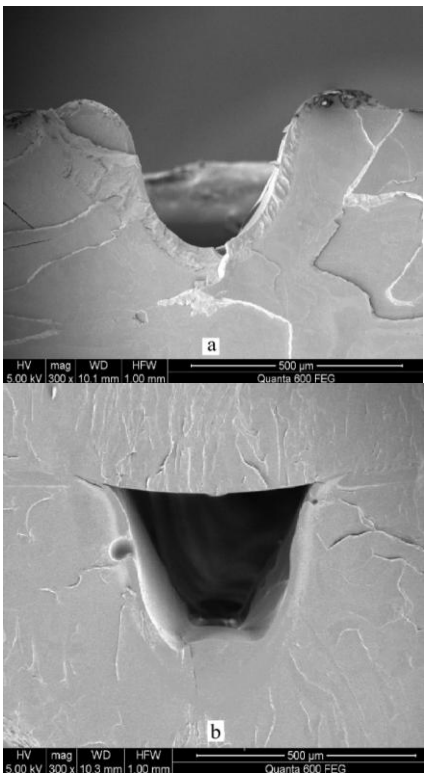

Fig. 7 The cross-section of the micromachnnel before (a) and after (b) bonding

2.4 Test of microfluidic droplet generator

Straight-line microchannels pattern as shown in Figure 8 was fabricated on the PS substrate, and the laser power and cutting speed were 11.25 W and 25 mm/s, respectively. The channels' depth is 308 µm and width is 324 µm. There are three inlet holes on the left and one outlet hole on the right. A polystyrene cover plate with four through holes at the corresponding positions was bonded to it at 102 ^{o}C for 120 minutes. The diameter of the inlet and outlet holes is a nominal 1.778 mm, matched to the tubing used. The tubing was first inserted into the holes, and then epoxy adhesive (MG Chemicals 8332-25ML) was applied surrounding the holes to seal it and avoid leakage of the fluids that will be injected into the channels.

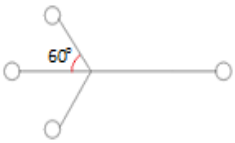

Fig. 8 Schematic microchannel pattern on PS substrate

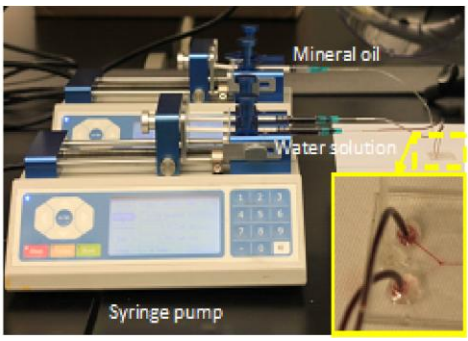

Fig. 9 Experimental setup for microfluidic droplets generator. The mineral oil and water solution of Cresol Red were injected simultaneously into the inlet tubing by separate syringe pumps

The system setup for droplet generation and test is shown in Figure 9. The purified DI water solution of Cresol Red was used as the dispersed phase in the continuous phase of mineral oil. The mineral oil was injected into the channel through the tubing that connected to the middle hole on the left, and the water solution of Cresol Red was injected into the channel through the tubing on both sides. The inside diameter and outside diameter of the flexible plastic tubing from Saint-Gobain Performance Plastics Corp. are 0.762 mm and 1.778 mm, respectively. The constant flow rates of the two immiscible fluids were controlled by syringe pumps (Fusion 200, CHEMYX INC.), and the flow rates were set to 0.01 ml/min for mineral oil and 0.005ml/min for the water solution of Cresol Red.

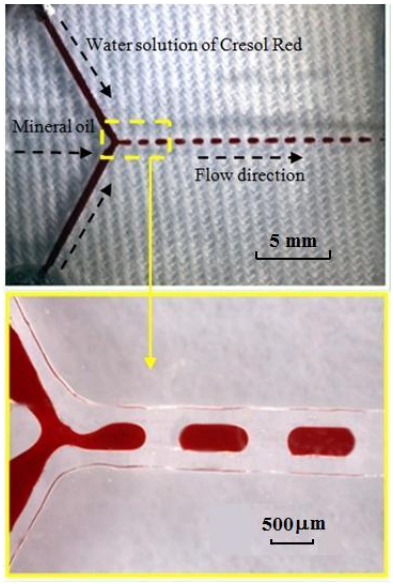

Fig. 10 Discrete droplets of water solution in continuous flow of mineral oil

The generated droplets of Cresol Red solution with the same size in the continuous mineral oil flow is shown in Figure 10. The droplets were generated by the shear force of the fluid flow, and the arc contour of the water droplets can be explained by the hydrophobic channel surface. The droplet size is controlled by the flow rate of the water solution while keeping the mineral oil flow rate constant, and slower flow rate of the water solution can generate smaller droplets.

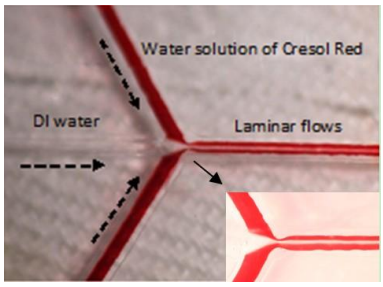

Fig. 11 Laminar flows in the polystyrene microfluidic device

Besides the droplets, laminar flows can also be generated by replacing the mineral oil in above

experiment with DI water that is miscible with Cresol Red solution, as shown in Figure 11, in which the flow rates of the DI water and water solution of Cresol Red were both set to 0.005 ml/min.

3 Conclusions

We have demonstrated a rapid method for the templateless formation of polystyrene microfluidic devices by using a CO_2 laser system, and it takes only several minutes to fabricate the patterning on the polystyrene substrate. The cost of this technique is low because it eliminates the necessary steps such as the mask fabrication, as well as corresponding microfabrication equipments and processes in conventional methods. The depth, width and aspect ratio of the microchannels depend on the laser power and cutting speed and the profile of the microchannels can be easily controlled. Although there are bumps as a result of surface tension driven flow on the cutting edge of the microchannels, they have no severe effect on the bonding process, and the polystyrene microfluidic devices have good performance to generate droplets. As a conclusion, this rapid and low cost method can be widely used for the rapid prototyping of polystyrene-based microfluidic devices.

References

Jakeway SC, Mello AJ, Russell EL (2000) Miniaturized total analysis systems for biological analysis. Fresenius' J Anal Chem 366 525-539

Nayak NC, Lam Y, Yue C, Sinha TA (2008) CO_2-laser micromachining of PMMA: the effect of polymer molecular weight. J Micromech Microeng 18: 095020

Link DR, Grasland-Mongrain E, Duri A, Sarrazin F, Cheng Z, Cristobal G, Marquez M, Weitz DA (2006) Electric Control of Droplets in Microfluidic Devices. Angew Chem Int Ed 118: 2618-2622

Fair RB (2007) Digital microfluidics: is a true lab-on-a-chip possible? Microfluid Nanofluid 3: 245-281

Duffy DC, McDonald JC, Schueller OJA, Whitesides GM (1998) Rapid Prototyping of Microfluidic Systems in Poly(dimethylsiloxane). Anal Chem 70: 4974-4984

Dolnik V, Liu SR, Jovanovich S (2000) Capillary electrophoresis on microchip. Electrophoresis 21: 41-54

Yao X, Chen Z, Chen G (2009) Fabrication of PMMA microfluidic chips using disposable agar hydrogel templates. Electrophoresis 30: 4225-4229

Reedy CR, Price CW, Sniegowski J, Ferrance JP, Begley M, Landers JP (2011) Solid phase extraction of DNA from biological samples in a post-based, high surface area poly(methyl methacrylate) (PMMA) microdevice. Lab Chip 11: 1603-1611

Darain F, Gan KL, Tjin SC (2009) Antibody immobilization on to polystyrene substrate—on-chip immunoassay for horse IgG based on fluorescence. Biomed Microdevices 11: 653-661

Young EWK, Berthier E, Guckenberger DJ, Sackmann E, Lamers C, Meyvantsson I, Huttenlocher A, Beebe DJ (2011) Rapid Prototyping of Arrayed Microfluidic Systems in Polystyrene for Cell-Based Assays. Anal Chem 83 1408-1417

Hoek I, Tho F, Arnold WM (2010) Sodium hydroxide treatment of PDMS based microfluidic devices. Lab Chip 10: 2283-2285

Pla-Roca M, Juncker D (2011) PDMS microfluidic capillary systems for patterning proteins on surfaces and performing miniaturized immunoassays. Methods in molecular biology (Clifton, NJ) 671: 177-194

Ogonczyk D, Wegrzyn J, Jankowski P, Dabrowski B, Garstecki P (2010) Bonding of microfluidic devices fabricated in polycarbonate. Lab Chip 10 1324-1327

Jankowski P, Ogonczyk D, Kosinski A, Lisowski W, Garstecki P (2011) Hydrophobic modification of polycarbonate for reproducible and stable formation of biocompatible microparticles. Lab Chip 11: 748-752

Chen CS, Breslauer DN, Luna J, Grimes A, Chin W, Lee L, Khine M (2008) Shrinky-Dink microfluidics: 3D polystyrene chips. Lab Chip 8: 622-624

Becker H, Gartner C (2000) Polymer microfabrication methods for microfluidic analytical applications. Electrophoresis 21: 12-26

Kaur J, Boro RC, Wangoo N, Singh KR, Suri CR (2008) Direct hapten coated immunoassay format for the detection of atrazine and 2,4-dichlorophenoxyacetic acid herbicides. Analytica Chimica Acta 607: 92-99

Martynova L, Locascio LE, Gaitan M, Kramer GW, Christensen RG, MacCrehan WA (1997) Fabrication of plastic microfluid channels by imprinting methods. Anal Chem 69 4783-4789

Gerlach A, Knebel G, Guber AE, Heckele M, Herrmann D, Muslia A, Sshaller T (2002) Microfabrication of single-use plastic microfluidic devices for high-throughput screening and DNA analysis. Microsyst Technol 7: 265-268

Rotting O, Ropke W, Becker H, Gartner C (2002) Polymer microfabrication technologies. Microsyst Technol 8: 32-36.

Lim CT, Low HY, Ng JKK, Liu WT, Zhang Y (2009) Fabrication of three-dimensional hemispherical structures using photolithography. Microfluid Nanofluid 7: 721-726

Urech L, Lippert T (2010) Photoablation of polymer materials. Photochemistry and Photophysics of Polymer Materials. John Wiley & Son Inc New York 541-568

Snakenborg D, Klank H, Kutter JP (2004) Microstructure fabrication with a CO2 laser system. J Micromech Microeng 14: 182-189

Yuan DJ, Das S (2007) Experimental and theoretical analysis of direct-write laser micromachining of polymethyl methacrylate by CO_2 laser ablation. J Appl Phys 101: 024901

Huang YG, Liu SB, Yang W, Yu CX (2010) Surface roughness analysis and improvement of PMMA-based microfluidic chip chambers by CO_2 laser cutting. Appl Surf Sci 256: 1675-1678

Liu HB, Gong HQ (2009) Templateless prototyping of polydimethylsiloxane microfluidic structures using a pulsed CO2 laser. J Micromech Microeng 19: 037002

Huft J, Da Costa DJ, Walker D, Hansen CL (2010) Three-dimensional large-scale microfluidic integration by laser ablation of interlayer connections. Lab Chip 10: 2358-2365

Qi H, Chen T, Yao LY, Zuo TC (2009) Micromachining of microchannel on the polycarbonate substrate with CO2 laser direct-writing ablation. Opt Laser Eng 47: 594-598

Tolstopyatov EM (2005) Ablation of polytetrafluoroet-hylene using a continuous CO_2 laser beam. J Phys D: Appl Phys 38: 1993-1999

Klank H, Kutter JP, Geschke O (2002) CO2-laser micromachining and back-end processing for rapid production of PMMA-based microfluidic systems. Lab Chip 2: 242-246

Huang SM, Sun Z, Luk'yanchuk BS, Hong MH, Shi LP (2005) Nanobump arrays fabricated by laser irradiation of polystyrene particle layers on silicon. Appl Phys Lett 86: 161911

Wu SH (1970) Surface and Interfacial Tensions of Polymer Melts. II. Poly(methyl methacrylate), Poly(n-butyl methacrylate) and Polystyrene. J Phys Chem 74: 632-638

Chen S C, Cahill DG, Grigoropoulos CP (2000) Melting and Surface Deformation in Pulsed Laser Surface Micromodification of Ni-P Disks. J Heat Transfer 122: 107-112